DOI: 10.1002/cssc.201200193

Role of Water in the Chlorine Evolution Reaction at RuO_2-Based Electrodes—Understanding Electrocatalysis as a Resonance Phenomenon

Aleksandar R. Zeradjanin,[a] Nadine Menzel,[b] Peter Strasser,[b] and Wolfgang Schuhmann*[a, c]

The reaction path of the Cl_2 evolution reaction (CER) was investigated by combining electrochemical and spectroscopic methods. It is shown that oxidation and reconstruction of the catalyst surface during CER is a consequence of the interaction between RuO_2 and water. The state of the RuO_2 surface during the electrochemical reaction was analyzed in situ by using Raman spectroscopy to monitor vibrations of the crystal lattice of RuO_2 and changes in the surface concentration of the adsorbed species as a function of the electrode potential. The role of the solvent was recognized as being crucial in the formation of an oxygen-containing hydrophilic layer, which is a key prerequisite for electrocatalytic Cl_2 formation. Water (more precisely the OH adlayer) is understood not just as a medium that allows adsorption of intermediates, but also as an integral part of the intermediate formed during the electrochemical reaction. New insights into the general understanding of electrocatalysis were obtained by utilizing the vibration frequencies of the crystal lattice as a dynamic catalytic descriptor instead of thermodynamic descriptors, such as the adsorption energy of intermediates. Interpretation of the derived "volcano" curve suggests that electrocatalysis is governed by a resonance phenomenon.

Introduction

Electrocatalytic gas-evolving reactions (GER), namely, chlorine (CER), hydrogen (HER), and oxygen evolution reactions (OERs), have been a matter of intensive investigation for decades.[1–13] Enormous technical significance[14] coupled with an insufficient fundamental understanding of GER motivated adequate unifying concepts in surface science to be established that could bridge electrochemistry with heterogeneous catalysis and surface physics.[12,15,16] Anodic GERs, such as the CER and OER, are particularly complicated for analysis where electron transfer proceeds at a reconstructed oxidized surface, which has properties that are substantially different from those at open-circuit conditions.

The effect of the electrode material on the electrode reaction rate, as discussed conventionally in electrocatalysis,[17] does not specify the impact of the solvent on the faradaic process at the electrode/electrolyte interface, whereas the theory of electron transfer postulates the importance of the solvent.[18] However, it is not fully understood how the solvent contributes to the rate of an electrode reaction,[1,19] especially if the reaction proceeds through adsorbed intermediates. In seminal papers by Trasatti[6,20] it was demonstrated that the work functions of metals in a solution are practically the same as those of metals in a vacuum. It was assumed that the solvent behaved like a dielectric continuum that shifted the absolute scale of reactivity to the same extent for all metals due to water dipoles, which alter the surface potential at the solid/liquid interface.[6]

Herein, we propose, based on spectro-electrochemical measurements, that the solvent, specifically in this case water, is crucial in the oxidation of Cl^- ions at RuO_2 electrodes, not only as a reaction medium, but also as an integral part of intermediates that allow electron transfer to take place as a prerequisite for the electrocatalytic reaction. Of particular importance is the observation that the electrocatalytic reaction is strongly dependent on characteristic vibrations in the catalyst crystals, leading to resonance phenomenon established between the electrode surface and intermediates in the electrochemical double layer.

Experimental Section

Cyclic voltammetry: Cyclic voltammetry was performed in a three-electrode setup at room temperature. The working electrode was a RuO_2-based dimensionally stable anode (DSA; Bayer Materials, Leverkusen, Germany) in the form of a chip with a diameter, d, of 1.5 cm. The exposed diameter, d_s, of the sample during analysis was 0.5 cm. The reference electrode was a homemade Ag/AgCl/3 M KCl electrode [0.207 V vs. a normal hydrogen electrode (NHE)]. The counter electrode was a Pt mesh. The Pt mesh and Ag wires were provided by Goodfellow (Bad Nauheim, Germany). A 3.5 M solution of NaCl (99.5%, J.T. Baker, Deventer, Netherlands) was used as the main electrolyte with HCl (37–38%, J.T. Baker, Deventer, Nether-

[a] A. R. Zeradjanin, Prof. Dr. W. Schuhmann
Analytische Chemie—Elektroanalytik & Sensorik
Ruhr-Universität Bochum
Universitätsstr. 150, 44780 Bochum (Germany)
[b] N. Menzel, Prof. Dr. P. Strasser
The Electrochemical Energy
Catalysis and Material Science Laboratory
Technische Universität Berlin
Straße des 17. Juni 124, 10623 Berlin (Germany)
[c] Prof. Dr. W. Schuhmann
Center for Electrochemical Sciences (CES)
Ruhr-Universität Bochum
Universitätsstr. 150, 44780 Bochum (Germany)

lands) added until a pH value of 3 was reached. For an estimation of the level of oxidation of the surface during CER, 1, 2, 3, and 4 M solutions of NaCl were used at a pH value of 2 maintained by addition of HCl, and the ionic strength was kept constant by using $NaNO_3$ (99%, Roth, Karlsruhe, Germany). All solutions were prepared with deionized water. The potential of the working electrode was controlled by a bipotentiostat/galvanostat (Jaissle PG 100, Waiblingen, Germany). Samples were pretreated by potential cycling as described elsewhere.[21]

Raman spectroscopy: Raman spectroscopy measurements were conducted with a Jobin–Yvon iHR550 spectrometer (Horiba, Germany) equipped with a thermoelectrically (TE)-cooled charge device. Excitation was achieved with a laser MPC 6000, Model Ventus LP (Laser Quantum, UK) instrument with a wavelength of 532 nm. The laser power was set to 10 mW. Experiments were conducted in air and in electrolyte at a temperature of 25 °C. The potential of the sample was controlled by means of a μAutolabIII/Fra2 potentiostat/galvanostat (EcoChemie, Utrecht, The Netherlands). Data processing was carried out by using OriginPro8G software (OriginLab, Northampton, USA).

Results and Discussion

Acid–base properties of RuO_2 as the basis of electrocatalytic activity

An important characteristic of some transition-metal oxides, including RuO_2, is their acid–base properties. Cyclic voltammetry was used for the analysis of surface properties of RuO_2.[22] In a range of electrode potentials at which water is thermodynamically stable, the hydrated form of RuO_2 can reversibly exchange protons with the electrolyte due to redox transitions, which are registered as pseudocapacitive currents. The charge exchanged during these processes is proportional to the number of active sites at the RuO_2 surface.[23–25] In the potential range from −0.150 to 1.05 V versus Ag/AgCl/3 M KCl, the only relevant process is protonation/deprotonation of RuO_2. This behavior is reversible, and the charge for deprotonation in the anodic sweep is approximately equal to the charge for protonation in the cathodic sweep (Figure 1). Reaction (1) represents the surface deprotonation/protonation reaction:

$$RuO_x(OH)_y + z\,H^+ + e^- \rightleftharpoons RuO_{x-z}(OH)_{y+z} \quad (1)$$

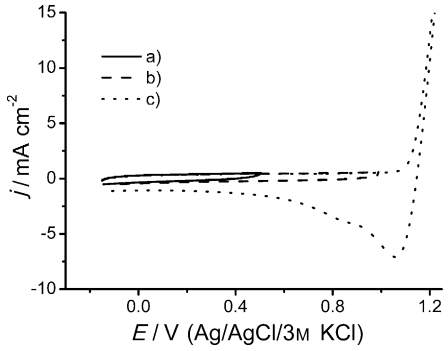

Figure 1. Cyclic voltammograms of RuO_2 electrodes in 3.5 M NaCl for three different anodic potential limits: a) −0.15 to 0.5 V; b) −0.15 to 1.0 V; and c) −0.15 to 1.2 V (3.5 M NaCl, pH 3, $v = 20\ mV\,s^{-1}$).

If the anodic polarization is extended above 1.05 V versus Ag/AgCl, the region of thermodynamic stability of water is exceeded and it is reasonable to assume that deprotonation of the solvent begins, consuming additional charge [Reaction (2)]:

$$H_2O \rightleftharpoons OH_{ad} + H^+ + e^- \quad (2)$$

In this case, the overall process is no longer reversible. Furthermore, a non-stoichiometric hydrated oxide can be deprotonated to form stoichiometric RuO_2 or even higher oxidation states, depending on the applied potential.

In addition to the deprotonation of water, according to Reaction (2), following the Brønsted–Lowry acid–base concept, acidification of the electrolyte near the electrode surface may be additionally caused by acceptance of an electron pair from the Cl^- ion, according to the Lewis acid–base concept [Reaction (3)]:

$$Cl^- \rightleftharpoons Cl_{ad} + e^- \quad (3)$$

Taking this into consideration, it is important to know the initial reaction step of the CER. If the CER commences by following Reaction (3), then Reaction (2) will decrease the selectivity of the overall reaction, leading to simultaneous OER. However, if the CER starts with Reaction (2), then Reaction (3) will block active sites at the catalyst surface.

Solvent-induced reaction pathway: Reconstruction of catalyst surface as prerequisite for CER

During anodic polarization above 1.05 V versus Ag/AgCl in a concentrated aqueous solution of NaCl, the OER and CER are expected to occur simultaneously. In fact, the OER is thermodynamically favored over the CER [Reaction (4)].

$$2\,Cl^- \rightleftharpoons Cl_2 + 2\,e^-$$
$$E^\circ = 1.15\ V\ vs.\ Ag/AgCl/3\ M\ KCl \quad (4a)$$
$$(t = 25\,^\circ C;\ a(Cl^-) = 1;\ p = 10^5\ Pa)$$

$$H_2O \rightleftharpoons O_2 + 4\,H^+ + 4\,e^-$$
$$E^\circ = 1.02\ V\ vs.\ Ag/AgCl/3\ M\ KCl \quad (4b)$$
$$(t = 25\,^\circ C;\ a(H^+) = 1;\ p = 10^5\ Pa)$$

At the same time, the CER is kinetically superior to the OER. The OER should already be negligible in 0.1 M NaCl.[26] However, it is known, on the other hand, that anodic water activation is the main source of corrosion of DSA,[27–31] essentially causing further oxidation of the oxide surface and the formation of unstable higher oxidation states of RuO_x.[32] From this perspective selectivity is considered to be of high importance. Taking into account that the CER is kinetically superior to the OER, it is suggestive that discharging of Cl^- ions dominates in concentrated NaCl solutions. However, reality seems to be much more complex.

It is important to establish correlations between the kinetics of the CER, as expressed by the exchange current density and

a number of parameters relevant for the intrinsic catalytic behavior. An increase in the rate of the CER may be caused by 1) a decrease in the dissociation energy of the metal–Cl bond, 2) a decrease in the d-band vacancy, or 3) a decrease in the amount of charge necessary for the oxidation of the surface during the CER.[33] The reasoning behind this is that metal centers with a large d-band vacancy, that is, a low electron density in the d band, are adsorbing strongly Cl^- ions or electron pairs from water molecules. While the d-band vacancy and the dissociation energy of the metal–Cl bond were utilized as catalytic descriptors, the amount of charge consumed for the oxidation of the catalyst surface during the CER was not yet focused upon.

One of the intriguing aspects of the CER and OER is the phenomenon of surface reconstruction. In these cases, the catalytically active layers are non-stoichiometric oxides and coordinatively unsaturated sites play a crucial role in the formation of intermediates.[10] Following the general understanding of anodic electrocatalytic reactions, the anion (Cl^-) or a molecule (H_2O) with a free electron pair(s) will be located in the inner Helmholtz plane, where the electronic density from the anion or molecule can be partially delivered to the d orbitals of the transition metal. Either of these two possibilities will cause the transformation of the existing RuO_x into a higher oxidation state during anodic polarization.

The enthalpy of bulk transition from a lower to a higher oxide is correlated with the kinetics of the OER and CER,[8] as well as with the binding energy between the oxide and adsorbed oxygen species.[10] However, to facilitate electrocatalytic reactions, it is important that the redox potential of the transition from the lower to the higher oxidation state of the metal oxide is close to the redox potential of the catalyzed reaction,[34,35] in this case the CER. In the case of metal centers with a large d-band vacancy, the redox potential of the transition from the lower to the higher oxidation state of the catalyst is too negative with respect to the redox potential of the CER. Thus, this redox transition of the catalyst occurs early and the surface is further oxidized with higher intensity during the reaction. This furthermore suggests the importance of the presence of water.

If water was not important for the CER, then it should be possible to obtain significant kinetics for the CER in Cl^--containing but nonaqueous solutions, providing that the catalytic material had a redox potential similar to the redox potential of the CER. However, it was demonstrated that the CER proceeded at a much lower rate, for example, when using trifluoroacetic acid as the solvent.[33] However, this result was derived exclusively from comparing the anodic current in trifluoroacetic acid with that in aqueous electrolytes. In a set of preliminary experiments we investigated the CER in a number of ionic liquids. No Cl_2 could be detected by means of differential electrochemical mass spectrometry (DEMS), despite anodic currents being measured upon anodic polarization of the electrode. The observed anodic currents originated from the formation of organochloro compounds.

Although most ionic liquids have lower dielectric constants than water,[36–39] Cl_2 should be produced in nonaqueous media if the contribution of the solvent were only due to electric field effects. Thus, the finding that no Cl_2 was detected further suggested a specific role of water in CER beyond that of just a solvent with a high dielectric constant.

To elucidate the possible influence of water on the CER, it is instructive to analyze one of the reaction pathways for the CER, as proposed by Erenburg.[40] [Reaction (5)]:

$$H_2O \rightleftharpoons OH_{ad} + H^+ + e^- \quad (5a)$$

$$OH_{ad} + Cl^- \rightleftharpoons HClO + e^- \quad \text{rate-determining step (rds) } b = 40\ \text{mV dec}^{-1} \quad (5b)$$

$$HClO + H^+ + Cl^- \rightleftharpoons Cl_2 + H_2O \quad (5c)$$

The proposed reaction pathway includes several discriminatory criteria, namely, that 1) water has to participate in the reaction; 2) the CER has to be pH dependent, with a partial order of the reaction of -1 with respect to the concentration of protons;[41] 3) the partial order of the reaction with respect to the Cl^- concentration is $+1$;[41] and 4) according to the value of the Tafel slope b of 40 mV dec^{-1}, the exchange of the second electron is rate determining.

In contrast, the usually assumed Volmer–Heyrovsky pathway[19,40] does not fulfill any of these criteria except 4). Clearly, any assumed reaction pathway for the CER, which starts with Cl^- discharging, cannot explain the observed pH dependence. As a matter of fact, any type of mechanistic analysis is essentially discriminatory. Thus, it merely leads to a suggestion concerning a higher probability of one reaction pathway over another. To additionally support the proposed reaction pathway, it is necessary, on the one hand, to get access to the nature of the adsorbed species (OH_{ad} or Cl_{ad}) present at the surface of RuO_2 and, on the other hand, to get variation of the surface coverage of the adsorbed species depending on the electrode potential.

In situ spectroscopic surface study of RuO_2 during CER

To get deeper insight into the electrode/electrolyte interface during the CER, Raman spectroscopy coupled with electrochemistry was used. The Raman spectra of a RuO_2-based DSA immersed in electrolyte solution at different electrode potentials are shown in Figure 2 over the wavelength range corresponding to the O–H stretching mode for both the O–H bond from surface water molecules or from OH adsorbed at the electrode surface. The most pronounced peak is at around 3470 cm^{-1}, with a shoulder at 3240 cm^{-1}, which decreases in intensity with increasing ionic strength of the solution.[42] The intensity of the peak corresponding to the O–H stretching mode decreases as the electrode potential becomes more positive (Figure 2). In other words, during acceleration of the CER due to the increasing potential, OH_{ad} or water molecules are readily deprotonated at the solid/liquid interface. No peak can be found in the Raman spectra in the range between 200 and 400 cm^{-1} that could be attributed to Cl_{ad} at the RuO_2 surface. Experiments at different Cl^- concentrations proved that only the shape of the peak of O–H stretching mode changed in the

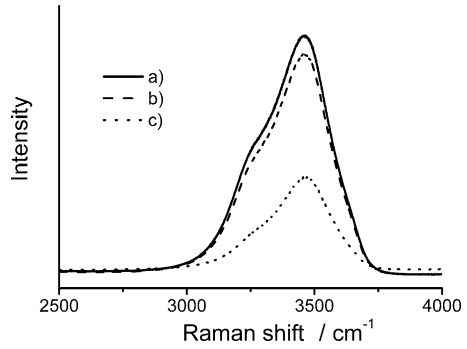

Figure 2. Raman spectra of TiO_2/RuO_2 in 3.5 M NaCl at pH 3 (addition of HCl) with increasing electrode potential: a) 1, b) 1.4, and c) 2.4 V. The peak of the O–H stretching mode is at a wavelength of around 3470 cm^{-1} with a shoulder at about 3240 cm^{-1}.

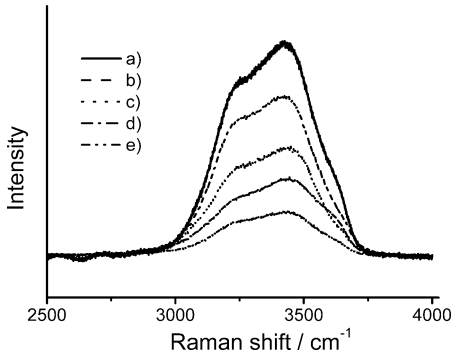

Figure 3. Raman spectra of the O–H stretching mode of water at electrode potentials of a) 1.2, b) 1.4, c 1.6, d) 1.8, and e) 2.0 V.

Raman spectra in agreement with the results given in Reference [42]. Clearly, the only relevant change in the surface concentration of species adsorbed at the electrode/electrolyte interface during the CER is associated with the solvent. This finding is seen as additional support for the proposed reaction pathway.

Clearly, Cl^- ions exclusively participate in the reaction pathway through an intermediate HClO complex formed with a surface-bound O, while simultaneously weakening the oxide/OH bond. The observed change in the intensity of the Raman spectra is due to a change in the coverage of adsorbed species and reflects deprotonation of water molecules (or OH_{ad}). The concentration of OH_{ad} should increase with increasing anodic polarization because Reaction (5b) is rate determining, and hence, slower than Reaction (5a). Taking into account the decrease in the O–H stretching mode intensity during acceleration of the CER (from 1 to 2.4 V vs. Ag/AgCl/3 M KCl), it becomes probable that even under open-circuit conditions water is substantially deprotonated. Thus, the reaction pathway most probably starts with deprotonation of OH_{ad} to form O_{ad} [Reaction (6a)]. In a subsequent step, HClO is formed as an intermediate [Reaction (6b)].

$$OH_{ad} \rightleftharpoons O_{ad} + H^+ + e^- \quad (6a)$$

$$O_{ad} + Cl^- + H^+ \rightleftharpoons HClO \quad (6b)$$

Reaction (6b) is immediately followed by Reaction (5c), while Reaction (6a) can alternatively proceed towards OER. It is important to note that the pathway according to Reactions (6a), (6b), and (5c) fulfills the four discriminatory criteria mentioned above derived from the evaluation of the Erenburg pathway.

Following the argument that Reaction (6a) should be the same for the OER and CER, we performed experiments in the absence of Cl^- to monitor the drop in OH_{ad} surface concentration (Figure 3). Due to the significantly lower reaction rate in the case of the OER, expected interference to the signal due to gas evolution was minimal. Figure 3 is very similar to the Raman spectra recorded in an aqueous solution of NaCl (cf. Figure 2); however, the shoulder at around 3240 cm^{-1} is more pronounced. From the proposed reaction path for the OER,[43] the final reaction is the recombination of two O_{ad}, which requires two active sites. In the case of the CER, if the reaction proceeds through HClO as an intermediate, only one active site is necessary to produce one Cl_2 molecule. This is seen as a potential reason for the facilitated kinetics of the CER compared with the OER.

Despite differences in the shape of the shoulder at 3240 cm^{-1}, it is necessary to detect HClO as an intermediate during CER to conclusively distinguish the CER from the OER by using Raman spectroscopy.

Matching of characteristic vibrations: Electrocatalysis as a resonance phenomenon

One of the fingerprints of RuO_2 in the Raman spectra is a peak at around 716 cm^{-1}, which corresponds to the B_{2g} vibration mode of RuO_2[44,45] considered to be a characteristic vibration of the crystal lattice of RuO_2. Figure 4 shows distinct changes in the Raman spectra at this wavelength with increasing anodic polarization if the spectrum is obtained in the absence or presence of Cl^- ions.

In the case of the Cl^--free aqueous electrolyte, a peak around 716 cm^{-1} slowly develops with increasing electrode potential (Figure 4A). In the presence of Cl^- ions in the electrolyte, this peak becomes substantially stronger (Figure 4B), invoking the question of why the B_{2g} vibration mode of RuO_2 is more pronounced during the CER than during the OER.

To understand the phenomenon of amplification of vibration modes of a crystal lattice, one has to ask what will allow a fast heterogeneous inner-sphere electron-transfer reaction to take place, which requires the existence of adsorbed intermediates. It is a common understanding that so-called "volcano" curves can be employed as a predictive basis.[17] Volcano curves usually express the kinetics of the electrode reaction as a function of a catalytic descriptor, such as the binding energy between the electrode surface and the adsorbed chemical species, which is an intermediate in the reaction pathway,[6] assuming that the highest kinetics is a function of the optimal value of the catalytic descriptor. The kinetics of the reaction is then expressed as a function of thermodynamic parameters. In other words, the physicochemical quantity of the process is ex-

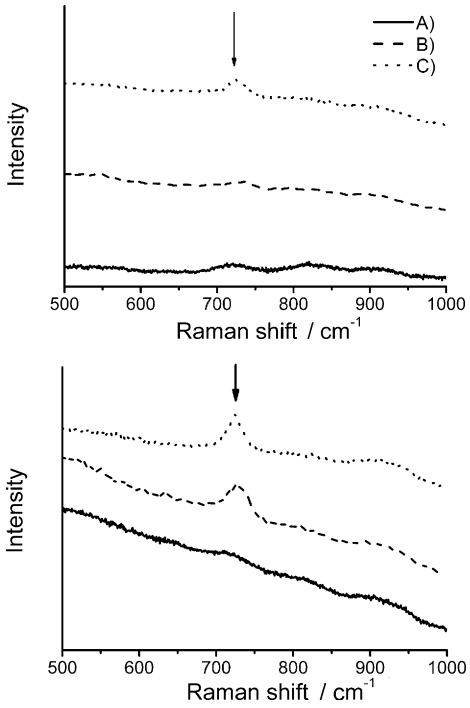

Figure 4. Raman spectra of a RuO_2-based DSA in water (upper image) and in 3.5 M NaCl (lower image), pH 3 (addition of HCl); applied potentials of A) 1, B) 1.4, and C) 2.4 V versus Ag/AgCl/3 M KCl were used.

spectra shown in Figure 4, probably due to the thickness of the electrolyte in this experiment. Hence, the experiments were repeated with a thinner electrolyte layer in the wavelength range from 400 and 1000 cm^{-1} (Figure 5).

In Figure 5 the characteristic peaks of RuO_2 (E_g) at 528 cm^{-1}, RuO_2 (B_{2g}) at 716 cm^{-1}, TiO_2 (B_{2g}) at 826 cm^{-1},[45] and RuO_4 (F_{2g}) 906 cm^{-1}[48] can be clearly distinguished in air as well as in the

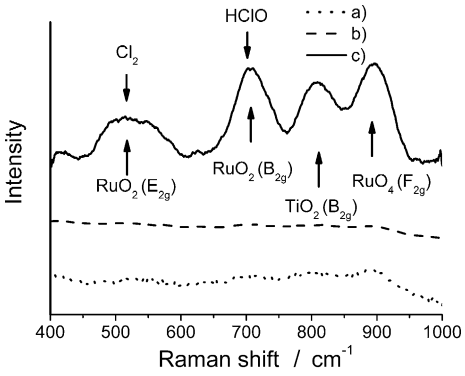

Figure 5. Raman spectra of a DSA (TiO_2/RuO_2) in a) air, b) in Cl^--containing electrolyte without polarization, and c) with the sample polarized at 1.5 V versus Ag/AgCl/3 M KCl in Cl^--containing electrolyte. The peaks at which characteristic vibrations of the RuO_2 lattice overlap with characteristic vibrations of chemical species (Cl_2 and HClO) in the solution are marked by arrows.

pressed as a function of the physicochemical quantity of the state. Even if we disregard the observations of Schmickler and Trasatti[46] and consider DFT predictions of electrocatalytic trends,[47] intuitively it is problematic to comprehend how one thermodynamic parameter can be sufficient to explain the dynamics of electron transfer at the electrode/electrolyte interface.

An electrochemical reaction as a process means that the chemical energy of an electron is transformed into electrical energy (or vice versa). If one understands an electron to be a tridimensional standing wave it represents a resonance vibration. This approach can also be used to describe the behavior of electrons when they are part of a chemical bond. The transfer of the vibrational energy of electrons into electrical current (or vice versa) proceeds through the electrical double layer. Taking into account that the timescales of electron transfer and molecular vibrations are similar, 10^{12}–10^{14} Hz, it is intriguing to comprehend the role of vibrational energy in electrocatalysis of the CER.

Keeping in mind previous observations concerning the activity trends of a number of potential catalysts for the CER,[8,10] additional insight is needed to explain why RuO_2 is an almost perfect catalyst for this specific reaction. There are four characteristic Raman vibration modes considered to be "fingerprints" of rutile RuO_2:[44,45] B_{1g} (97), E_g (528), A_{1g} (646), B_{2g} (716 cm^{-1}). The wavelength of 97 cm^{-1} is in a section of the Raman spectra below 200 cm^{-1} that is usually disregarded. The influence of the presence of Cl^- ions on the fourth band, at around 716 cm^{-1}, was already shown above (Figure 4). However, the vibrations at 528 and 646 cm^{-1} were not clearly visible in the Cl^--containing electrolyte solution. Upon polarizing the DSA to a potential of 1.5 V, all peaks become more pronounced, including, surprisingly, the TiO_2 peak. Considering the value of the potential for zero charge of the RuO_2/TiO_2 mixed oxide,[49] the water molecules are oriented with the oxygen towards electrode in the double layer at open-circuit potential. Thus, depending on the binding energy between the electrode and oxygen from water, a certain potential difference at the solid/liquid interface establishes which is modulated by the externally applied potential. The existence of RuO_4 during the reaction is of particular importance because it is proof of the oxidation of the surface as well as of the reconstruction of the surface during the CER. Hence, the redox transition of RuO_2 into a higher oxidation state occurs simultaneously with the CER. More generally, for successful inner-sphere electron transfer, the redox transition from a lower to higher oxidation state of the oxide, which is used as a catalyst, should proceed at a potential slightly more negative than the potential at which oxidation of the reactants occurs.[34]

The observation that the Raman shifts of HClO and Cl_2 in aqueous solution are 728 and 540 cm^{-1}, respectively,[50] and thus, very close to the Raman peaks of RuO_2 (Figure 5), is intriguing. Especially interesting is the match of the Raman shifts of HClO, the potential intermediate in the rate-determining step in the reaction pathway according to Erenburg, and the B_{2g} vibration mode of RuO_2. Moreover, the Raman shift of the product Cl_2 itself matches the E_g vibration mode of RuO_2. To evaluate whether this matching of the Raman vibrations was accidental, the Raman spectra of a range of oxides used or tested as potential catalysts for the CER were analyzed.

Interestingly, oxides that exhibit good electrocatalytic activity for the CER have a similar fingerprint in their Raman spectra as RuO_2. The closer the vibrational modes are to those observed for RuO_2 the better the catalytic performance of the oxide. This suggests a correlation of the kinetics of the CER with the characteristic Raman frequencies as an electrocatalytic descriptor.

The lack of accurate experimental data for overpotentials or exchange current densities in the case of the CER can be overcome by rationalization of existing data for the OER because the general activity trend for the CER and OER is almost identical for a number of transition-metal oxides. When the potential for the OER is plotted as a function of the potential for the CER for the same current density, a slope equal to one is observed.[8] This suggests that the use of kinetic data for the OER[8] can be used to analyze activity trends qualitatively in the case of CER for a range of oxides. The overpotential for the CER is always lower than that for the OER. The volcano curve in the case of the OER is constructed from the dependence of the overpotential, at a defined current density, on the enthalpy of the transition from the lower to the higher oxidation state of the oxide,[8] or more recently, on the oxygen chemisorption energy on the catalyst surface.[11]A linear dependence between the surface potential of water at an electrode and the enthalpy of oxide formation of a metal has already been established for several metals.[51] This implicitly suggests that the rate of reaction for the CER is connected to the enthalpy of the lower/higher oxide transition, which is then directly connected to the nature and strength of the interaction between oxide and oxygen from the water molecule. According to Rossmeisl et al.,[10] the binding energy between the metal ion in the oxide and O_{ad} is a universal catalytic descriptor for the CER and OER.

Finally, the overpotentials for several transition-metal oxides with the same current density[8] are expressed as a function of the characteristic Raman shifts (Figure 6).

Evidently, the kinetics of the CER exhibits a volcano-type dependence on the characteristic Raman shift (Figure 6). This is qualitatively a different volcano curve from that previously plotted for the OER (or any other electrode reaction) because the catalytic descriptor is the Raman shift, which is a dynamic property based on the vibrations of chemical bonds. Additionally, a further qualitative difference is seen in the fact that the maximum of the volcano curve at 725 cm^{-1} corresponds to the vibration of the Cl–O bond in an aqueous solution of free HClO. On one hand, this additionally suggests that HClO is the most likely intermediate in the CER. However, even more importantly, this supposes that the optimal catalyst for the CER should exhibit a vibration of the M–O bond in the oxide identical to the vibration of Cl–O bond in the HClO intermediate. Even more intriguingly, the vibrations of the bond cleaved or formed during a catalytic reaction have to be in resonance with the vibrational modes of the catalyst surface. The first indication of similar conclusions was recently given by Koper, assuming a Volmer–Heyrovsky reaction pathway in the case of the CER.[19] On an ideal catalyst, the intermediate Cl_{ad} is just as strongly bound to the catalyst surface as it is in the Cl_2 molecule. This can be interpreted as a connection between surface binding energy and free energy in a molecule.

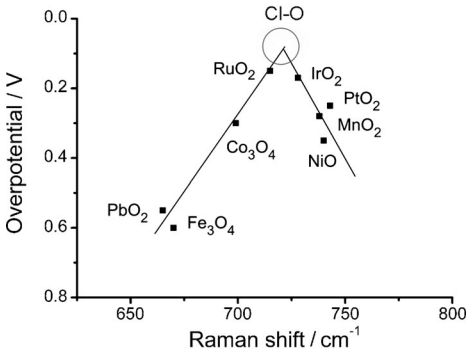

Figure 6. Overpotentials of the CER as a function of the characteristic Raman shifts. The top of the volcano curve marked with the circle corresponds to the Raman shift of the Cl–O bond vibration of HClO in aqueous solution. The values of the overpotentials for the CER were taken from Reference [8], whereas values for Raman shifts of RuO_2, IrO_2, PtO_2, MnO_2, Co_3O_4, NiO, PbO_2, and Fe_3O_4 were taken from References [45, 52–58], respectively.

Moreover, Raman spectroscopy can provide an understanding of why the CER starts with water discharging. From Raman spectra it can be derived that the Cl–O bond is stronger than the Cl–Cl bond. Thus, instead of replacing an adsorbed water molecule with Cl_{ad}, it is much more probable that Cl^- will attach to an oxygen site from an oriented water dipole or to OH_{ad} because the Cl–O bond is stronger than the M–Cl bond. In accordance with Reference [19] the Cl–Cl bond is approximately twice as strong as the M–Cl_{ad} bond.

The length of the M–O bond is inversely proportional to the Raman stretching frequency. Excellent agreement can be achieved between Raman spectroscopy and X-ray absorption near-edge spectroscopy (XANES) for an estimation of the M–O bond lengths.[59] Thus, in addition to identifying the best catalyst for a particular reaction, it should be possible to calculate, using characteristic vibrational frequencies, the optimal interatomic distance, M–O, the vibration of which will match the vibration of the intermediate, allowing facilitated electron transfer. This may become important because it allows the possibility of tuning the properties of low-cost metal oxides with the intention of imitating vibrational modes of expensive oxides, which are known as good catalysts.

Qualitative relationship between resonance and binding energy during electrocatalytic reactions

To further discuss the proposed concept, the volcano curve of the most studied reaction in electrochemistry, the HER was analyzed. The maximum of the volcano curve for the optimum catalyst is obtained if the change in the free energy during establishing or breaking of the M–H bond is equal to zero.[6,47] This implies that the binding energy, which is essentially the enthalpy of bond formation between the surface and intermediate, is defined by the change in entropy.

If $\Delta G = 0$, then $\Delta H = T\Delta S$, which means that, in the case of an optimum catalyst, the binding energy between the surface and the adsorbed species is determined by the entropy change. As a matter of fact, this suggests a strong impact of

the solvent on the rate of the reaction. This is in agreement with the Marcus theory,[18] in which the reorganization energy of the solvent is seen as a crucial factor determining the activation energy for outer-sphere reactions. The above-discussed concept now suggests that, in inner-sphere reactions, such as the HER, the solvent also has a major impact on the reaction rate in the case of an optimum catalyst. The entire process of adsorption of a specific ion, for example, a proton from solution consists of three steps, namely, desolvation of the ion, which leads to an increase in entropy; desorption of the water molecule(s), which leads to a further increase in entropy; and finally adsorption of the desolvated ion, which causes a decrease in entropy. The change in degrees of freedom during the adsorption is $3n-3$, in which n represents the number of solvent molecules, due to the loss of three translational degrees of freedom. In an ideal case ($n=1$), the increase in entropy during solvent desorption is equal to the decrease of entropy during ion adsorption, leading to a situation where the entire process would be driven by the entropy of the desolvation of the ion. Hence, if the adsorption process is driven by the entropy of desolvation of the ion, at least a qualitative link between the optimum binding energy of the intermediate and reorganization energy of the solvent is suggested.

If we now apply these considerations to the CER, elucidation of why the maximum of the volcano curve derived from the characteristic Raman vibrations (Figure 6) corresponds to the Cl–O vibration in bulk solution instead of the Cl–O vibration of the surface bound species remains to be determined. The maximum of the volcano curve should correlate with the optimum binding energy or Raman frequency of the adsorbed intermediate in the rate-determining step. However, as shown in Figure 6, the maximum of the volcano curve corresponds to the Raman frequency of HClO in solution (725 cm^{-1}). Thus, the difference of the Cl–O vibration frequency of HClO in solution and the vibration frequency of Cl–O in HClO attached to the surface has to be evaluated. In case of an optimal catalyst, no free energy was consumed for establishing or breaking of the OM–OCl bond and the reaction was exclusively entropy driven. In that case, no particular change in the vibrational frequency can be expected when considering that the vibrational frequency is defined by the chemical energy stored in a particular chemical bond. Thus, if the vibrational frequency of the M–O bond in the oxide is similar or equal to that of the Cl–O bond of the adsorbed intermediate, the exchange of electrons through the O–M–O–Cl adsorbate will happen most efficiently in accordance with the Frank–Condon principle. During an electronic transition, a change from one vibrational energy level to another will be more likely to happen if the two vibrational wavefunctions overlap more significantly; this is the basis of the equation for the reaction rate introduced by Levitch and Dogonadze.[35] Moreover, if during the formation of the OM–OCl bond and the exchange of electrons, the O–M bond oscillates with a similar frequency to that of the Cl–O bond, a resonance phenomenon will be established, leading to a very intensive oscillation until either bond breaking occurs or the bond is weak enough that HClO can be replaced by a "new" water molecule or OH_{ad}. Conclusively, one can assume that, for the optimum catalyst, the difference in the characteristic vibration frequency of the Cl–O bond in solution and at the surface is close to zero.

Conclusions

The acid–base properties of RuO_2 are recognized as the foundation for the catalytic properties in the OER and CER. Unavoidable oxidation of RuO_2 is not only a consequence of the anodic activation of water, but is indispensably necessary for efficient CER and OER due to the concomitant reconstruction of the surface.

Raman spectroscopy combined with electrochemistry confirmed that the surface was covered with OH_{ad} and not with Cl_{ad} as previously assumed. Raman spectroscopy at increasing electrode potentials furthermore confirmed that HClO was a crucial intermediate for the catalytic reaction. The vibrational modes of the crystal lattice of RuO_2 were very similar to the vibration of the Cl–O bond in HClO dissolved in water. The assumed oxidation of the surface was confirmed by Raman spectroscopy, and the formation of RuO_4 suggested the necessity for a redox transition from lower to higher oxidation states of the ruthenium oxide during the electrocatalytic process. Finally, a volcano curve was derived by using a dynamic catalytic descriptor, namely, the characteristic vibration of the M–O bond, for which the maximum of the volcano curve corresponded to the vibration of the Cl–O bond in HClO.

In summary, the following points are important for the electrocatalytic CER:

1) Cl^- ions are transported into the double layer by the applied electrode potential where they react with O_{ad} and form HClO as an intermediate. The vibration frequency in the Cl–O bond is very similar to the vibration frequency of the M–O bond of the oxide.
2) The frequency of vibration of the Cl–Cl bond in the final product is very similar to the second vibrational mode of the M–O bond of the oxide.
3) Efficient electron transfer during the electrocatalytic reaction will occur if the redox transition from lower to higher oxidation states is performed at a potential slightly lower than the electrode potential of the electrocatalytic reaction.
4) Electrocatalysis of the CER is recognized as a resonance phenomenon between the catalyst surface, intermediates, and products where the vibrations of chemical bonds occur with a similar frequency.

Acknowledgements

We are grateful to the BMBF in the framework of the project "Innovative Technologien für Ressourceneffizienz rohstoffintensiver Produktionsprozesse: Effizienzsteigerung bei der Chlor-Herstellung" (FKZ: 033R018E). Special thanks go to Dr. Stefanie Schwamborn for help with Raman spectroscopy.

Keywords: electrochemistry · gas-evolving reactions · Raman spectroscopy · reaction mechanisms · solvent effects

[1] J. O'M. Bockris, *Nature* **1946**, *158*, 584.
[2] J. O'M. Bockris, *Nature* **1947**, *159*, 539.
[3] J. O'M. Bockris, *Nature* **1947**, *159*, 401.
[4] B. E. Conway, B. V. Tilak, *Electrochim. Acta* **2002**, *47*, 3571.
[5] R. Parsons, *Trans. Faraday Soc.* **1958**, *54*, 1053.
[6] S. Trasatti, *J. Electroanal. Chem.* **1972**, *39*, 163.
[7] A. T. Kuhn, C. J. Mortimer, G. C. Bond, J. Lindley, *J. Electroanal. Chem.* **1972**, *34*, 1.
[8] S. Trasatti, *Electrochim. Acta* **1984**, *29*, 1503.
[9] J. O'M. Bockris, T. Otagawa, *J. Electrochem. Soc.* **1984**, *131*, 290.
[10] H. A. Hansen, I. C. Man, F. Studt, F. Abild-Pedersen, T. Bligaard, J. Rossmeisl, *Phys. Chem. Chem. Phys.* **2010**, *12*, 283.
[11] I. C. Man, H. Y. Su, F. Calle-Vallejo, H. A. Hansen, J. I. Martínez, N. G. Inoglu, J. Kitchin, T. J. Jaramillo, J. K. Nørskov, J. Rossmeisl, *ChemCatChem* **2011**, *3*, 1159.
[12] H. Dau, C. Limberg, T. Reier, M. Risch, S. Roggan, P. Strasser, *ChemCatChem* **2010**, *2*, 724.
[13] J. Suntivich, K. J. May, H. A. Gasteiger, J. B. Goodenough, S.-Y. Horn, *Science* **2011**, *334*, 1383.
[14] EuroChlor (representing the chloro–alkali industry), *Chlorine Industry Review* **2007–2008**.
[15] C. G. Vayenas, *J. Solid State Electrochem.* **2011**, *15*, 1425.
[16] A. R. Zeradjanin, F. La Mantia, J. Masa, W. Schuhmann, *Electrochim. Acta*, in press DOI: 10.1016/j.electacta.2012.04.101.
[17] S. Trasatti, *Electrochim. Acta* **2000**, *45*, 2377.
[18] R. A. Marcus, *Annu. Rev. Phys. Chem.* **1964**, *15*, 155.
[19] M. T. M. Koper, *J. Electroanal. Chem.* **2011**, *660*, 254.
[20] S. Trasatti, *J. Electroanal. Chem.* **1971**, *33*, 351.
[21] J. Mozota, M. Vukovic, B. E. Conway, *J. Electroanal. Chem.* **1980**, *114*, 153.
[22] C. Angelinetta, S. Trasatti, Lj. D. Atanasoska, Z. S. Minevski, R. T. Atanasoski, *Mater. Chem. Phys.* **1989**, *22*, 231.
[23] L. D. Burke, O. J. Murphy, *J. Electroanal. Chem.* **1980**, *112*, 39.
[24] L. D. Burke, O. J. Murphy, J. F. O'Neill, *J. Electroanal. Chem.* **1977**, *81*, 391.
[25] L. D. Burke, O. J. Murphy, *J. Electroanal. Chem.* **1979**, *96*, 19.
[26] S. Ardizzone, A. Carugati, G. Lodi, S. Trasatti, *J. Electrochem. Soc.* **1982**, *129*, 1689.
[27] B. V. Tilak, V. I. Birss, J. Wang, C. P. Chen, S. K. Rangarajand, *J. Electrochem. Soc.* **2001**, *148*, D112.
[28] A. S. Pilla, E. O. Cobo, M. M. E. Duarte, D. R. Salinas, *J. Appl. Electrochem.* **1997**, *27*, 1283.
[29] G. N. Martellia, R. Ornelasa, G. Faitaa, *Electrochim. Acta* **1994**, *39*, 1551.
[30] S. M. Hoseinieh, F. Ashrafizadeh, M. H. Maddahi, *J. Electrochem. Soc.* **2010**, *157*, E50.
[31] S. V. Evdokimov, *Russ. J. Electrochem.* **2000**, *36*, 231.
[32] Lj. M. Gajić-Krstajić, T. Lj. Trišović, N. V. Krstajić, *Corros. Sci.* **2004**, *46*, 65.
[33] P. Gu, Ph.D thesis, University of Otawa (Canada), **1990**, pp. 23, 141.
[34] A. C. C. Tseung, S. Jasem, *Electrochim. Acta* **1977**, *22*, 31.
[35] Y. Matsumoto, E. Sato, *Mater. Chem. Phys.* **1986**, *14*, 397.
[36] K. E. Johnson, *ECS Interface* **2007**, *16*, 38.
[37] M. M. Huang, Y. Jiang, P. Sasisanker, W. G. Driver, H. Weingärtner, *J. Chem. Eng. Data* **2011**, *56*, 1494.
[38] T. Singh, A. Kumar, *J. Phys. Chem. B* **2008**, *112*, 12968.
[39] C. Wakai, A. Oleinikova, M. Ott, H. Weingärtner, *J. Phys. Chem. B* **2005**, *109*, 17028.
[40] S. Trasatti, *Electrochim. Acta* **1987**, *32*, 369.
[41] V. Consonni, S. Trasatti, F. Pollak, W. E. O'Grady, *J. Electroanal. Chem.* **1987**, *228*, 393.
[42] R. Li, Z. Jiang, Y. Guam, H. Yang, B. Liu, *J. Raman Spectrosc.* **2009**, *40*, 1200.
[43] P. Castelli, S. Trasatti, F. H. Pollak, W. E. O'Grady, *J. Electroanal. Chem.* **1986**, *210*, 189.
[44] S. Y. Mar, C. S. Chen, Y. S. Huang, K. K. Tiong, *Appl. Surf. Sci.* **1995**, *90*, 497.
[45] Y. S. Huang, F. H. Pollak, *Solid State Commun.* **1982**, *43*, 921.
[46] T. Schmickler, S. Trasatti, *J. Electrochem. Soc.* **2006**, *153*, L31.
[47] J. K. Nørskov, T. Bliigard, A. Logadottir, J. R. Kitchin, J. G. Chen, S. Pandelov, U. Stimming, *J. Electrochem. Soc.* **2005**, *152*, J23.
[48] W. P. Griffith, *J. Chem. Soc. A* **1968**, 1663.
[49] L. A. De Faria, S. Trasatti, *J. Electroanal. Chem.* **1992**, *340*, 145.
[50] S. Nakagawara, T. Goto, M. Nara, Y. Ozawa, K. Hotta, Y. Arata, *Anal. Sci.* **1998**, *14*, 691.
[51] S. Trasatti, *J. Electroanal. Chem.* **1974**, *54*, 437.
[52] Y. S. Huang, S. S. Lin, C. R. Huang, M. C. Lee, T. E. Dann, F. Z. Chien, *Solid State Commun.* **1989**, *70*, 517.
[53] W. H. Weber in *Raman Scattering in Materials Science* (Eds.: W. H. Weber, R. Merlin), Springer, Berlin, **2000**, Chap. 6, pp. 249.
[54] C. Julien, M. Massot, S. Rangan, M. Lemal, D. Guyomard, *J. Raman Spectrosc.* **2002**, *33*, 223.
[55] V. G. Hadjiev, M. N. Iliev, I. V. Vergilov, *J. Phys. C* **1988**, *21*, L199.
[56] E. Cazzanelli, A. Kuzmin, G. Mariotto, E. Mironova-Ulmane, *J. Phys. Condens. Matter* **2003**, *15*, 2045.
[57] L. Burgio, R. J. H. Clark, S. Firth, *Analyst* **2001**, *126*, 222.
[58] O. N. Shebanova, P. Lazor, *J. Raman Spectrosc.* **2003**, *34*, 845.
[59] I. Wachs, *Catal. Today* **1996**, *27*, 437.

Received: March 17, 2012
Published online on August 14, 2012

